Adiabatic elimination for ensembles of emitters in cavities with dissipative couplings

D. Hagenmüller,[1] S. Schütz,[1] G. Pupillo,[1] and J. Schachenmayer[1,2,*]
[1]*Université de Strasbourg and CNRS, ISIS (UMR 7006), and icFRC, 67000 Strasbourg, France*
[2]*IPCMS (UMR 7504), CNRS, 67000 Strasbourg, France*

(Received 7 April 2020; accepted 22 June 2020; published 14 July 2020)

We consider an ensemble of cavity-coupled two-level emitters interacting via full (coherent and dissipative) dipole-dipole interactions. We detail an adiabatic elimination procedure to derive effective equations of motion for a subsystem consisting of the cavity and a single emitter and analyze limitations of effective subsystem parameters. We study how joint dissipative decay processes in the subsystem affect cavity-coupling properties of the single emitter and cavity transmission spectra.

DOI: 10.1103/PhysRevA.102.013714

I. INTRODUCTION

The strong-coupling regime of cavity QED is reached when an excitation in matter can exchange energy with a confined mode of the electromagnetic field at a rate faster than losses [1–3]. In this case, hybrid light-matter normal modes called polaritons with frequencies shifted from the bare resonances are formed. Since the first pioneering experiments with atoms [4–6], there has been a growing interest in the possibility of modifying the fundamental properties of condensed matter systems by harnessing strong coupling to a cavity-type structure [7–17]. However, strong coupling is generally impeded by either weak dipole moments or large losses, and finding strategies to overcome these issues is therefore of fundamental importance in the field. In this context, recent experiments have demonstrated that strong coupling of a target oscillator playing an important role in certain chemical reactions or in the onset of superconductivity can be achieved by exploiting an "active" environment consisting of auxiliary oscillators that are strongly coupled to cavity photons and quasiresonant with the target oscillator [18,19].

In Ref. [20], we proposed a general scheme to collectively enhance the coupling of a single quantum emitter (A) to a cavity mode via the presence of a nearby ensemble of emitters (B) that couple to both the cavity and A. In experimental systems, reaching strong coupling for a single emitter can often be very difficult because of the requirement of small mode volumes of the cavity with large quality factors. A common path to reach strong coupling has been to simultaneously couple a large number N of emitters to the same mode, which leads to a collective coupling strength enhancement by a factor $\sqrt{N}$. Unfortunately, collective coupling does not lead to an enhanced photon-blockade effect, i.e., a nonlinear quantum effect for the cavity mode [21–23]. The latter effect would be desirable for photonic quantum information processing [24]. In Ref. [20] we proposed a mechanism of how a collective effect can still lead to an enhanced photon nonlinearity, simply by increasing the number of surrounding emitters B. There, we have demonstrated a viable path for a strong collective enhancement of the coupling strength of a single silicon-vacancy center to a microcavity. This may lead to new possibilities for engineering quantum information applications based on photon nonlinearities in such systems. Reference [20] further emphasizes the crucial role that active environments can play in cavity-QED experiments [18,19].

In the first part of this work, we present the detailed procedure for the microscopic adiabatic elimination of ensemble B from Ref. [20], either when the latter is far detuned from A or when the decay rates of the B emitters are the largest parameters of the problem. We show that the dissipative couplings of A to B can lead to effective coherent Hamiltonian terms within the subsystem $\mathcal{S}$ consisting of A and the cavity that can help to reach strong coupling. We compare results from the full adiabatic elimination vs the one where the emitters are treated in a linear classical approach. While the general effect of dissipatively engineered coherent interactions has been well studied for quantum information applications [25–30], here we explain how dissipative couplings can be exploited in cavity QED. As an additional feature to Ref. [20], in the second part we analyze the limitations of achievable effective parameters in subsystem $\mathcal{S}$ and its effective collective dissipative dynamics. Specifically, here we discuss the impact of effective collective decay processes on the cavity transmission spectrum and the onset of strong coupling.

The paper is organized as follows: In Sec. II, we introduce our model and describe the quantum master equation for the full system consisting of A, B, and the cavity. In Sec. III we derive in detail the effective master equation for subsystem $\mathcal{S}$. We first use an extension of the method given in [31] for the general situation where dissipative couplings between A and B are also present and derive the effective master equation parameters (Sec. III A). We then show that the same effective parameters appear in a linear classical approach valid in the low excitation limit (Sec. III B). In Sec. IV we discuss the limitations of the effective parameters of the subsystem and their dependence on the geometry. Therefore, we analyze the case where B can be reduced to an effective single emitter (Sec. IV A) and provide analytical formulas for the modification of the parameters in this case. We then focus on

*johannes.schachenmayer@gmail.com

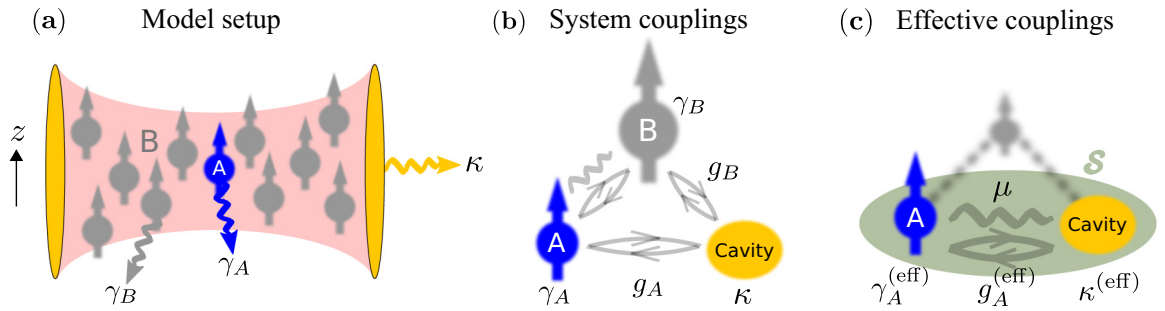

FIG. 1. (a) Sketch of the model setup: A single quantum emitter A (decay rate γ_A) and an ensemble of nearby emitters B (decay rates γ_B) are coupled to a cavity mode (decay rate κ). (b) Schematics of couplings: A and B couple to the cavity with the respective coherent Hamiltonian terms $\propto g_A$ and $\propto g_B$ (rounded arrows). The emitters interact among each other via dipole-dipole interactions with both Hamiltonian (rounded arrows) and dissipative (wavy line) terms. (c) Schematics of couplings in subsystem $\mathcal{S}$ after adiabatic elimination of B: The presence of B modifies $\gamma_A \to \gamma_A^{(\mathrm{eff})}$ and $\kappa \to \kappa^{(\mathrm{eff})}$. Effective couplings in the subsystem comprise both coherent [$g_A \to g_A^{(\mathrm{eff})}$] and dissipative ($\mu$) couplings.

the consequences of collective decay processes of A and the cavity (Sec. IV B), which effectively appear after the adiabatic elimination of B. Finally, we provide a conclusion and an outlook in Sec. V.

II. MODEL

We consider a single two-level emitter A (level spacing ω_A, decay rate γ_A), an ensemble B consisting of N emitters (each with level spacing ω_B, decay rate γ_B), and a cavity mode (frequency ω_c, decay rate κ) [see Fig. 1(a); $\hbar \equiv 1$ throughout this paper]. All emitters are coupled to the cavity and interact with each other via dipole-dipole interactions (the dipole direction is chosen along the z axis). In a frame rotating with ω_A, the full quantum master equation for the density matrix ρ of the system can be written as

$$\partial_t \rho = -i[H_0 + H_{\mathrm{TC}} + H_{\mathrm{DD}}, \rho] + \mathcal{L}\rho. \tag{1}$$

Here, the Hamiltonian parts include the bare system energies,

$$H_0 = \Delta_c a^\dagger a + \sum_{j=1}^{N} \Delta_B \sigma_j^+ \sigma_j^-, \tag{2}$$

with $\Delta_c = \omega_c - \omega_A$ and $\Delta_B = \omega_B - \omega_A$. The bosonic operators a and $a^\dagger$ annihilate and create a photon in the cavity, while $\sigma_A^\pm$ and $\sigma_j^\pm$ are the spin ladder operators for A and for the jth emitter of ensemble B, respectively. The emitter-cavity interaction is governed by a Tavis-Cummings Hamiltonian [1,32],

$$H_{\mathrm{TC}} = a^\dagger \left(g_A \sigma_A^- + \sum_{j=1}^{N} g_j \sigma_j^- \right) + \mathrm{H.c.}, \tag{3}$$

with respective coupling strengths g_A and g_j. The dipole-dipole interaction Hamiltonian is given by [33,34]

$$H_{\mathrm{DD}} = \sum_{j=1}^{N} \Omega_{jA} (\sigma_j^+ \sigma_A^- + \sigma_A^+ \sigma_j^-) + \sum_{j \neq \ell}^{N} \Omega_{j\ell} \sigma_j^+ \sigma_\ell^-, \tag{4}$$

with Ω_{jA} denoting the coupling strengths between A and the jth spin of B, and $\Omega_{j\ell}$ the coupling strengths between pairs of emitters within B.

Dissipation in Eq. (1) is described by the superoperator

$$\mathcal{L}\rho = -\kappa \mathcal{D}(a^\dagger, a)\rho - \gamma_A \mathcal{D}(\sigma_A^+, \sigma_A^-)\rho + \mathcal{L}_{\mathrm{BB}}\rho + \mathcal{L}_{\mathrm{AB}}\rho, \tag{5}$$

with $\mathcal{D}(x, y)\rho = [x, y\rho] + [\rho x, y]$. The dissipator given by $\mathcal{L}_{\mathrm{BB}}\rho = -\sum_{j,\ell=1}^{N} \gamma_{j\ell} \mathcal{D}(\sigma_j^+, \sigma_\ell^-)\rho$ describes collective decay processes within the B ensemble, and $\gamma_{jj} = \gamma_B$. Additionally,

$$\mathcal{L}_{\mathrm{AB}}\rho = -\sum_{j=1}^{N} \gamma_{jA} (\mathcal{D}(\sigma_j^+, \sigma_A^-)\rho + \mathcal{D}(\sigma_A^+, \sigma_j^-)\rho) \tag{6}$$

describes dissipative couplings between A and B [see Fig. 1(b) for a sketch of the couplings].

In this work we are interested in deriving effective equations of motions for the density matrix of subsystem $\mathcal{S}$ consisting of A and the cavity after adiabatically eliminating B [see Fig. 1(c)]. As we show below, besides energy shifts, these equations feature modified decay rates [$\gamma_A \to \gamma_A^{(\mathrm{eff})}$ and $\kappa \to \kappa^{(\mathrm{eff})}$], as well as modified couplings between A and the cavity. The latter consist of both coherent Jaynes-Cummings-type couplings [with an effective coupling strength $g_A \to g_A^{(\mathrm{eff})}$] as well as collective dissipation terms with rate μ.

III. DERIVATION OF THE EFFECTIVE QUANTUM MASTER EQUATION

In this section, we derive the effective quantum master equation obtained when the emitter ensemble B is adiabatically eliminated, which leads to modified physical parameters for subsystem $\mathcal{S}$ [Fig. 1(c)]. The main results are the effective master equation parameters provided in Sec. III A 6. The derivation of the parameters is split into two parts. In Sec. III A we utilize a full adiabatic elimination procedure similar to that in Ref. [31]. In Sec. III B we show that the same effective parameters also appear in a classical linear theory for low spin excitations.

A. Full adiabatic elimination procedure

Our derivation of the effective master equation in this section relies on elimination techniques (see, e.g., [35–38]) and is based on a projection method given in Ref. [31], which we extend to the general case where dissipative dipole-dipole

couplings between A and B (i.e., $\mathcal{S}$ and B) are also present. This method relies on the projection of the density operator onto the ground-state manifold of B (Sec. III A 1), suitable decompositions of the master equation and the density operator (Sec. III A 2 and Sec. III A 3), followed by second-order perturbation theory in the interaction between $\mathcal{S}$ and B (Sec. III A 4) and time-scale separation (Sec. III A 5). The main results of the adiabatic elimination are the effective parameters for the subsystem $\mathcal{S}$ master equation and are provided in Sec. III A 6.

1. Projection onto the ground-state manifold

We assume that the set $\{|s_i\rangle\}$ forms a basis for subsystem $\mathcal{S}$, while $\{|b_i\rangle\}$ is a basis for the interacting ensemble B. The density operator ρ of the full system can be written as $\rho = \sum_{ijkl} \rho_{ij;kl} |s_i\rangle\langle s_j| \otimes |b_k\rangle\langle b_l|$ with matrix elements $\rho_{ij;kl} = \langle s_i, b_k|\rho|s_j, b_l\rangle$ and $|s_j, b_l\rangle = |s_j\rangle \otimes |b_l\rangle$. We are interested in the time evolution of the reduced density operator $\rho^{\text{eff}} = \sum_{ij} \rho^{\text{eff}}_{ij} |s_i\rangle\langle s_j|$ of $\mathcal{S}$ obtained by taking the partial trace $\text{Tr}_B \rho = \sum_m \langle b_m|\rho|b_m\rangle$ over the B ensemble, where $\rho^{\text{eff}}_{ij} = \sum_m \rho_{ij;mm}$ involves a sum over all possible basis states of B.

We assume that state $|g\rangle$ with *all* spins of B in their ground states mainly contributes to the latter sum and, therefore, introduce the superoperator $P\bullet = |g\rangle\langle g| \bullet |g\rangle\langle g|$ as a projector onto the elements of interest of the density operator ρ with $P\rho = \rho_{gg}|g\rangle\langle g|$ and $\rho_{gg} = \langle g|\rho|g\rangle$. In the following, we derive an equation for the time evolution of $v = P\rho$. Under the assumption that the spins of B remain close to their ground states, we derive the effective time evolution for the reduced density operator ρ^{eff} of $\mathcal{S}$ with $\rho^{\text{eff}} \approx \rho_{gg}$.

2. Decomposition of the master equation

We start by decomposing the full quantum master equation, (1), for the total density operator ρ as

$$\partial_t \rho = \mathfrak{L}\rho = (\mathcal{L}_S + \mathcal{L}_B + J + \mathcal{L}_{\text{int}})\rho. \tag{7}$$

The first term

$$\mathcal{L}_S \rho = -i[H_S, \rho] + \mathcal{L}_A \rho + \mathcal{L}_c \rho \tag{8}$$

is associated with the dynamics in $\mathcal{S}$, which includes the coherent evolution governed by the Hamiltonian $H_S = \Delta_c a^\dagger a + g_A(\sigma_A^+ a + a^\dagger \sigma_A^-)$, as well as a coupling to the environment associated with the terms $\mathcal{L}_A \rho = -\gamma_A(\sigma_A^+ \sigma_A^- \rho + \rho \sigma_A^+ \sigma_A^- - 2\sigma_A^- \rho \sigma_A^+)$ for spin A and $\mathcal{L}_c \rho = -\kappa(a^\dagger a \rho + \rho a^\dagger a - 2a\rho a^\dagger)$ for the cavity mode.

The second term reads

$$\mathcal{L}_B \rho = -i\vec{\sigma}_+^{\,\text{T}} \mathbf{M} \vec{\sigma}_- \rho + i\rho \vec{\sigma}_+^{\,\text{T}} \mathbf{M}^* \vec{\sigma}_-. \tag{9}$$

Here, we have used vector and matrix notations (a superscript T denotes the transpose operation) with

$$(\mathbf{M})_{j\ell} = (\Delta_B - i\gamma_B)\delta_{j\ell} + (1 - \delta_{j\ell})(\Omega_{j\ell} - i\gamma_{j\ell}) \tag{10}$$

and the spin ladder operators of B $(\vec{\sigma}_\pm)_j = \sigma_j^\pm$. The matrix $\mathbf{M}$ describes the internal dynamics of the B ensemble, namely, the free evolution $\sim\Delta_B$ of each spin of B, their couplings to the environment $\sim\gamma_B$, and their mutual interactions due to coherent ($\sim\Omega_{j\ell}$) and incoherent ($\sim\gamma_{j\ell}$) dipole-dipole interactions.

The third term in Eq. (7) reads

$$J\rho = 2\vec{\sigma}_-^{\,\text{T}} \boldsymbol{\gamma} \rho \vec{\sigma}_+ \tag{11}$$

and includes both individual (diagonal) and correlated (off-diagonal) terms for the ensemble B with $(\boldsymbol{\gamma})_{j\ell} = \gamma_{j\ell}$.

The last term in Eq. (7) is given by

$$\begin{aligned}\mathcal{L}_{\text{int}}\rho =& -i[(a\vec{G}^{\text{T}} + \sigma_A^- \vec{V}^{\text{T}})\vec{\sigma}_+ + (a^\dagger \vec{G}^{\text{T}} + \sigma_A^+ \vec{V}^{\text{T}})\vec{\sigma}_-]\rho \\ &+ i\rho[(a\vec{G}^{\text{T}} + \sigma_A^- \vec{V}^{*\text{T}})\vec{\sigma}_+ + (a^\dagger \vec{G}^{\text{T}} + \sigma_A^+ \vec{V}^{*\text{T}})\vec{\sigma}_-] \\ &+ 2(\sigma_A^- \rho(\vec{\gamma}^{\,\text{T}}\vec{\sigma}_+) + (\vec{\gamma}^{\,\text{T}}\vec{\sigma}_-)\rho\sigma_A^+)\end{aligned} \tag{12}$$

and describes the coupling of B to A and to the cavity mode. Here, we have introduced the vector notations $(\vec{G})_j = g_j$ and $\vec{V} = \vec{\Omega} - i\vec{\gamma}$ with $(\vec{\Omega})_j = \Omega_{jA}$ and $(\vec{\gamma})_j = \gamma_{jA}$. While coherent spin-cavity and spin-spin couplings are encoded in $\vec{G}$ and $\vec{\Omega}$, respectively, the terms $\propto \vec{\gamma}$ describe the dissipative part of the spin-spin coupling between A and B. The latter constitute a dissipative coupling between $\mathcal{S}$ and B.

3. Decomposition of the density operator

With the convenient form of Eq. (7), we can now decompose the total density operator as

$$\rho = (P + Q)\rho = v + w, \tag{13}$$

with $w = Q\rho = (1 - P)\rho$, and derive an equation of motion for the projection $v = \rho_{gg}|g\rangle\langle g|$ of the density operator onto the ground-state manifold of B. The projectors P and Q fulfill the relations $P^2\rho = P\rho$, $Q^2\rho = Q\rho$, and $PQ\rho = QP\rho = 0$. Using Eq. (7), the time evolution of the operators v and w is given by $\partial_t v = P(\partial_t \rho) = P\mathfrak{L}P\rho + P\mathfrak{L}Q\rho$ and $\partial_t w = Q(\partial_t \rho) = Q\mathfrak{L}P\rho + Q\mathfrak{L}Q\rho$. One can show that among all possibilities stemming from the different contributions to $\mathfrak{L}$, the only nonvanishing terms are

$$\begin{aligned}&P\mathfrak{L}P = P\mathcal{L}_S P, \quad P\mathfrak{L}Q = PJQ + P\mathcal{L}_{\text{int}}Q, \\ &Q\mathfrak{L}P = Q\mathcal{L}_{\text{int}}P, \quad Q\mathfrak{L}Q = Q(\mathcal{L}_S + \mathcal{L}_B + J + \mathcal{L}_{\text{int}})Q.\end{aligned} \tag{14}$$

Henceforth, we assume that

$$\begin{aligned}w = Q\rho \simeq &\sum_j \langle g|\rho|e_j\rangle |g\rangle\langle e_j| + \sum_j \langle e_j|\rho|g\rangle |e_j\rangle\langle g| \\ &+ \sum_{j,l} \langle e_j|\rho|e_l\rangle |e_j\rangle\langle e_l|,\end{aligned} \tag{15}$$

i.e., we restrict the following calculations to the single-excitation subspace where the B ensemble contains at most one excitation, consistently with the assumption that the spins of B remain close to their ground states. Here, $|e_j\rangle$ denotes the state where the jth spin of B is in its excited state, while the others are in their ground states. This approximation allows us to discard the term $QJQ \sim 0$ in Eq. (14). In total, the equations of motion of the projected density operators then read

$$\partial_t v = P\mathcal{L}_S v + P(J + \mathcal{L}_{\text{int}})w, \tag{16}$$

$$\partial_t w = Q(\mathcal{L}_B + \mathcal{L}_S)w + Q\mathcal{L}_{\text{int}}v + Q\mathcal{L}_{\text{int}}w. \tag{17}$$

Introducing the operator $\mathcal{L}_0 = \mathcal{L}_S + \mathcal{L}_B$ that describes the free evolution of the system, the formal solution of Eq. (17) is

$$w(t) = e^{Q\mathcal{L}_0(t-t_0)}w(t_0) + \int_{t_0}^{t} d\tau e^{Q\mathcal{L}_0(t-\tau)}[Q\mathcal{L}_{\rm int}v(\tau) + Q\mathcal{L}_{\rm int}w(\tau)], \quad (18)$$

which we now insert into Eq. (16). This yields

$$\begin{aligned}\partial_t v = {} & P\mathcal{L}_S v + P(J+\mathcal{L}_{\rm int})\int_{t_0}^{t} d\tau e^{Q\mathcal{L}_0(t-\tau)}Q\mathcal{L}_{\rm int}v(\tau) \\ & + P(J+\mathcal{L}_{\rm int})\int_{t_0}^{t} d\tau e^{Q\mathcal{L}_0(t-\tau)}Q\mathcal{L}_{\rm int} \\ & \times \int_{t_0}^{\tau} d\tau' e^{Q\mathcal{L}_0(\tau-\tau')}[Q\mathcal{L}_{\rm int}v(\tau') + Q\mathcal{L}_{\rm int}w(\tau')], \quad (19)\end{aligned}$$

assuming that the B ensemble is initially in its ground state $[w(t_0) = 0]$.

Equation (19) is the desired equation of motion for the projection v of the density operator onto the ground-state manifold of B. In the following sections, we evaluate the different contributions entering this equation using the definitions in Sec. III A 2, as well as a perturbative expansion in $\mathcal{L}_{\rm int}$ which describes the couplings of B to A and to the cavity mode.

4. Perturbation to second order in $\mathcal{L}_{\rm int}$

We now consider all possible processes up to second order in $\mathcal{L}_{\rm int}$. This procedure consists of a perturbative treatment of the interaction between A and the cavity mode with the quasimodes of the interacting B ensemble. It is justified when the coupling strengths of these quasimodes to subsystem $\mathcal{S}$ is sufficiently small compared to their (far-detuned) eigenfrequencies or dissipation rates (see, e.g., the Appendix), which ensures that the spins of B remain weakly excited. Up to second order in $\mathcal{L}_{\rm int}$, Eq. (19) provides

$$\begin{aligned}\partial_t v = {} & P\mathcal{L}_S v + P\mathcal{L}_{\rm int}\int_{0}^{t-t_0} d\tau e^{Q\mathcal{L}_0\tau}Q\mathcal{L}_{\rm int}v(t-\tau) \\ & + PJ\int_{0}^{t-t_0} d\tau e^{Q\mathcal{L}_0\tau}Q\mathcal{L}_{\rm int} \\ & \times \int_{0}^{t-t_0-\tau} d\tau' e^{Q\mathcal{L}_0\tau'}Q\mathcal{L}_{\rm int}v(t-\tau-\tau'). \quad (20)\end{aligned}$$

Note that we have neglected the term $Q\mathcal{L}_{\rm int}w(\tau')$ in Eq. (19) since its contribution is at least of order $O(\mathcal{L}_{\rm int}^3)$ [see Eq. (18)]. Furthermore, our truncation is also consistent with neglecting the term QJQ in Eq. (14) as we did before since the latter would provide contributions of higher order in $\mathcal{L}_{\rm int}$. In order to calculate the different contributions entering Eq. (20), it is convenient to use a spectral decomposition of the $N \times N$ non-Hermitian, complex symmetric matrix $\mathbf{M}$ in Eq. (10). Assuming that the latter can be diagonalized [39], we write $\mathbf{B} \equiv -i\mathbf{M}$ and $\mathbf{B} = \sum_j \lambda_j \vec{x}_j \vec{x}_j^{\rm T}$, where λ_j and $\vec{x}_j$ $(j = 1, \ldots, N)$ denote the complex eigenvalues and eigenvectors of $\mathbf{B}$, respectively. The eigenvectors satisfy the completeness relation $\sum_j \vec{x}_j \vec{x}_j^{\rm T} = \mathbf{1}$ and form an orthogonal basis with respect to the inner product $\vec{x}_j^{\rm T}\vec{x}_\ell = \delta_{j,\ell}$.

5. Integration using time-scale separation

We can now proceed with the integration of the different terms entering Eq. (20) and first calculate quantities of the type $\mathcal{L}_{\rm int}e^{Q\mathcal{L}_0\tau}Q\mathcal{L}_{\rm int}v(t-\tau)$. Using the definitions Eq. (12) and $v(t) = \rho_{gg}(t)|g\rangle\langle g|$, as well as the completeness relation, we obtain

$$\mathcal{L}_{\rm int}v(t-\tau) = -i\sum_j V_j^{\uparrow}\rho_{gg}(t-\tau)|x_j\rangle\langle g| + \text{H.c.}, \quad (21)$$

where $V_j^{\uparrow} = (a\vec{G}^{\rm T} + \sigma_A^-\vec{V}^{\rm T})\vec{x}_j$ describes the action on subsystem $\mathcal{S}$ when an excitation $|x_j\rangle = (\vec{x}_j^{\rm T}\vec{\sigma}_+)|g\rangle$ for the jth eigenmode of B is created.

Under the assumption that the dynamics of subsystem $\mathcal{S}$ is slow compared to the internal dynamics of B, one can use $\rho_{gg}(t-\tau) \approx \rho_{gg}(t)$ in the integrand of Eq. (20), together with a Taylor expansion to zeroth order in $\mathcal{L}_S\tau$ of the operator $\exp[Q\mathcal{L}_S\tau]Q$, such that $\exp[Q(\mathcal{L}_B+\mathcal{L}_S)\tau]Q \approx \exp[Q\mathcal{L}_B\tau]Q$. Using the relation $\mathcal{L}_B|x_j\rangle\langle g| = \lambda_j|x_j\rangle\langle g|$, we obtain

$$e^{Q\mathcal{L}_0\tau}Q\mathcal{L}_{\rm int}v(t-\tau) \approx -i\sum_j e^{\lambda_j\tau}V_j^{\uparrow}\rho_{gg}(t)|x_j\rangle\langle g| + \text{H.c.} \quad (22)$$

Now applying $\mathcal{L}_{\rm int}$ to the previous expression (while restricting ourselves to the single-excitation subspace) leads to

$$\begin{aligned}& \mathcal{L}_{\rm int}Q\left(-i\sum_j e^{\lambda_j\tau}V_j^{\uparrow}\rho_{gg}(t)|x_j\rangle\langle g| + \text{H.c.}\right) \\ & = -(a^\dagger\vec{G}^{\rm T} + \sigma_A^+\vec{V}^{\rm T})\vec{\sigma}_-\sum_j e^{\lambda_j\tau}V_j^{\uparrow}\rho_{gg}(t)|x_j\rangle\langle g| + \text{H.c.} \\ & \quad - 2i(\vec{\gamma}^{\rm T}\vec{\sigma}_-)\sum_j e^{\lambda_j\tau}V_j^{\uparrow}\rho_{gg}(t)|x_j\rangle\langle g|\sigma_A^+ + \text{H.c.} \\ & \quad + \sum_j e^{\lambda_j\tau}V_j^{\uparrow}\rho_{gg}(t)|x_j\rangle\langle g|(a^\dagger\vec{G}^{\rm T} + \sigma_A^+(\vec{V}^*)^{\rm T})\vec{\sigma}_- + \text{H.c.}\end{aligned} \quad (23)$$

Integration of the previous expression according to Eq. (20) provides terms proportional to $1 - e^{\lambda_j(t-t_0)} \approx 1$. This is justified when the expression is averaged on a coarse-grained time scale Δt [40,41] that fulfills $|\lambda_j|^{-1} \ll \Delta t \ll \tau_s$, with τ_s^{-1} the typical rate for the dynamics of subsystem $\mathcal{S}$. Note that, e.g., $\text{Re}[\lambda_1] = -\gamma_B < 0$ for a single B.

We now use the completeness relation once again, as well as the relations $P(\vec{x}_j^{\rm T}\vec{\sigma}_-)(\vec{x}_\ell^{\rm T}\vec{\sigma}_+)|g\rangle\langle g| = \delta_{j\ell}|g\rangle\langle g|$ and $\sum_j \vec{x}_j\vec{x}_j^{\rm T}/\lambda_j = \mathbf{B}^{-1}$, in such a way that the second term in the first line of Eq. (20) becomes

$$\begin{aligned}& P\mathcal{L}_{\rm int}\int_0^{t-t_0} d\tau e^{Q\mathcal{L}_0\tau}Q\mathcal{L}_{\rm int}v(t-\tau) \\ & \approx i([\vec{G}^{\rm T}\mathbf{M}^{-1}\vec{G}]a^\dagger a + [\vec{G}^{\rm T}\mathbf{M}^{-1}\vec{V}]a^\dagger\sigma_A^- \\ & \quad + [\vec{V}^{\rm T}\mathbf{M}^{-1}\vec{G}]\sigma_A^+ a + [\vec{V}^{\rm T}\mathbf{M}^{-1}\vec{V}]\sigma_A^+\sigma_A^-)v(t) + \text{H.c.} \\ & \quad - 2([\vec{\gamma}^{\rm T}\mathbf{M}^{-1}\vec{G}]av(t)\sigma_A^+ + [\vec{\gamma}^{\rm T}\mathbf{M}^{-1}\vec{V}]\sigma_A^- v(t)\sigma_A^+) + \text{H.c.}\end{aligned} \quad (24)$$

The third term in Eq. (20) is calculated similarly, first using $\rho_{gg}(t-\tau-\tau') \approx \rho_{gg}(t-\tau)$ together with $\exp[Q\mathcal{L}_0\tau'] \approx \exp[Q\mathcal{L}_B\tau']$ and then $\rho_{gg}(t-\tau) \approx \rho_{gg}(t)$ with $\exp[Q\mathcal{L}_0\tau] \approx \exp[Q\mathcal{L}_B\tau]$. Moreover, we use

$$\mathcal{L}_B|x_j\rangle\langle x_k^*| = (\lambda_j + \lambda_k^*)|x_j\rangle\langle x_k^*| \tag{25}$$

with $\langle x_k^*| = \langle g|(\vec{x}_k^{*T}\vec{\sigma}_-)$ and exploit the relations $2\vec{x}_j^{\mathrm{T}}\boldsymbol{\gamma}\vec{x}_\ell^* = -(\lambda_j + \lambda_\ell^*)\vec{x}_j^{\mathrm{T}}\vec{x}_\ell^*$ and $\vec{X}^{\mathrm{T}}\mathbf{M}^{-1}\vec{V}^* = \vec{X}^{\mathrm{T}}\mathbf{M}^{-1}\vec{V} + 2i\vec{X}^{\mathrm{T}}\mathbf{M}^{-1}\vec{\gamma}$ with $\vec{X} = \vec{G}, \vec{V}$. Averaging over a coarse-grained time scale Δt, we finally obtain

$$\begin{aligned} PJ\int_0^{t-t_0} d\tau e^{Q\mathcal{L}_0\tau}Q\mathcal{L}_{\mathrm{int}}\int_0^{t-t_0-\tau} d\tau' e^{Q\mathcal{L}_0\tau'}Q\mathcal{L}_{\mathrm{int}}v(t-\tau-\tau') \\ \approx -i([\vec{G}^{\mathrm{T}}\mathbf{M}^{-1}\vec{G}]av(t)a^\dagger + [\vec{G}^{\mathrm{T}}\mathbf{M}^{-1}\vec{V}]av(t)\sigma_A^+ \\ + [\vec{V}^{\mathrm{T}}\mathbf{M}^{-1}\vec{G}]\sigma_A^- v(t)a^\dagger + [\vec{V}^{\mathrm{T}}\mathbf{M}^{-1}\vec{V}]\sigma_A^- v(t)\sigma_A^+) + \mathrm{H.c.} \\ + 2([\vec{G}^{\mathrm{T}}\mathbf{M}^{-1}\vec{\gamma}]av(t)\sigma_A^+ + [\vec{V}^{\mathrm{T}}\mathbf{M}^{-1}\vec{\gamma}]\sigma_A^- v(t)\sigma_A^+) + \mathrm{H.c.} \end{aligned} \tag{26}$$

Now that the second and third terms on the right-hand side of Eq. (20) have been calculated [Eqs. (24) and (26), respectively], we can gather these contributions to write Eq. (20) in the usual master equation form with new effective parameters.

6. Effective master equation parameters

Using the property $\vec{X}^{\mathrm{T}}\mathbf{M}^{-1}\vec{Y} = \vec{Y}^{\mathrm{T}}\mathbf{M}^{-1}\vec{X}$ $(\vec{X}, \vec{Y} = \vec{G}, \vec{V})$ for the symmetric matrix $\mathbf{M}$, the effective master equation reads

$$\partial_t v = \mathfrak{L}^{\mathrm{eff}}v = -i\big[H_0^{\mathrm{eff}} + H_{\mathrm{JC}}^{\mathrm{eff}}, v\big] + \mathcal{L}^{\mathrm{eff}}v, \tag{27}$$

with the effective Hamiltonians

$$H_0^{\mathrm{eff}} = \Delta_A^{\mathrm{eff}}\sigma_A^+\sigma_A^- + \Delta_c^{\mathrm{eff}}a^\dagger a, \tag{28}$$

$$H_{\mathrm{JC}}^{\mathrm{eff}} = g_A^{\mathrm{eff}}(a^\dagger\sigma_A^- + \sigma_A^+ a) \tag{29}$$

and the effective dissipator

$$\begin{aligned} \mathcal{L}^{\mathrm{eff}}v = &-\kappa^{\mathrm{eff}}\mathcal{D}(a^\dagger, a)v - \gamma_A^{\mathrm{eff}}\mathcal{D}(\sigma_A^+, \sigma_A^-)v \\ &- \mu(\mathcal{D}(a^\dagger, \sigma_A^-)v + \mathcal{D}(\sigma_A^+, a)v). \end{aligned} \tag{30}$$

Here, the effective parameters are

$$\begin{aligned} \Delta_c^{\mathrm{eff}} &= \Delta_c - \mathrm{Re}[\vec{G}^{\mathrm{T}}\mathbf{M}^{-1}\vec{G}], \quad \Delta_A^{\mathrm{eff}} = -\mathrm{Re}[\vec{V}^{\mathrm{T}}\mathbf{M}^{-1}\vec{V}], \\ g_A^{\mathrm{eff}} &= g_A - \mathrm{Re}[\vec{G}^{\mathrm{T}}\mathbf{M}^{-1}\vec{V}], \quad \kappa^{\mathrm{eff}} = \kappa + \mathrm{Im}[\vec{G}^{\mathrm{T}}\mathbf{M}^{-1}\vec{G}], \\ \gamma_A^{\mathrm{eff}} &= \gamma_A + \mathrm{Im}[\vec{V}^{\mathrm{T}}\mathbf{M}^{-1}\vec{V}], \quad \mu = \mathrm{Im}[\vec{G}^{\mathrm{T}}\mathbf{M}^{-1}\vec{V}]. \end{aligned} \tag{31}$$

Here, dissipative couplings between A and B (and thus $\mathcal{S}$ and B) are encoded in $\vec{\gamma} = -\mathrm{Im}[\vec{V}]$.

Note that since the emitters of the eliminated ensemble B are supposed to remain close to their ground states (low spin excitations), the same derivation can be carried out when B consists of bosonic degrees of freedom instead of spins.

The effective master equation parameters in Eq. (31) are the main result of the adiabatic elimination procedure. In Sec. IV below, we analyze those parameters for various situations.

B. Elimination in the classical limit

We now show that the parameters from Eq. (31) are identical to parameters that appear in a linear classical model for the limit of low excitation numbers. The equations of motion for the expectation values of the photon annihilation operator a and the spin-lowering operators σ_A^- and σ_j^- are derived from Eq. (1) as [42]

$$\partial_t\langle a\rangle = -i(\Delta_c - i\kappa)\langle a\rangle - ig_A\langle\sigma_A^-\rangle - i\sum_j g_j\langle\sigma_j^-\rangle, \tag{32}$$

$$\partial_t\langle\sigma_A^-\rangle = -\gamma_A\langle\sigma_A^-\rangle - ig_A\langle a\rangle - \sum_j(\gamma_{jA} + i\Omega_{jA})\langle\sigma_j^-\rangle, \tag{33}$$

$$\begin{aligned} \partial_t\langle\sigma_j^-\rangle = &-i(\Delta_B - i\gamma_B)\langle\sigma_j^-\rangle - ig_j\langle a\rangle \\ &- (\gamma_{jA} + i\Omega_{jA})\langle\sigma_A^-\rangle - \sum_{\ell\neq j}(\gamma_{j\ell} + i\Omega_{j\ell})\langle\sigma_\ell^-\rangle, \end{aligned} \tag{34}$$

under the assumption of low-spin excitations $[\sigma_A^-, \sigma_A^+] \approx 1$ and $[\sigma_\ell^-, \sigma_\ell^+] \approx 1$ [43]. Note that since these equations of motion describe coupled harmonic oscillators, this method can alternatively be used when considering another cavity or a mechanical oscillator for B and/or A (see, for instance, Refs. [44] and [45]).

It is convenient to introduce the notations $\alpha \equiv \langle a\rangle$, $\beta_A \equiv \langle\sigma_A^-\rangle$, and $\vec{\beta} \equiv \langle\vec{\sigma}_-\rangle$, which allows us to write the previous set of equations in the compact form

$$\partial_t\alpha = -i[\Delta_c - i\kappa]\alpha - ig_A\beta_A - i\vec{G}^{\mathrm{T}}\vec{\beta}, \tag{35}$$

$$\partial_t\beta_A = -i[-i\gamma_A]\beta_A - ig_A\alpha - i\vec{V}^{\mathrm{T}}\vec{\beta}, \tag{36}$$

$$\partial_t\vec{\beta} = -i\mathbf{M}\vec{\beta} - i\vec{G}\alpha - i\vec{V}\beta_A, \tag{37}$$

where $\vec{G}$ and $\vec{V}$ are defined in Sec. III A 2. Equation (37) admits the steady-state solution

$$\vec{\beta} = -\mathbf{M}^{-1}\vec{G}\alpha - \mathbf{M}^{-1}\vec{V}\beta_A. \tag{38}$$

Now using the solution Eq. (38) in Eqs. (35) and (36) one obtains

$$\begin{aligned} \partial_t\alpha &= -i\big[\Delta_c^{\mathrm{eff}} - i\kappa^{\mathrm{eff}}\big]\alpha - i\big[g_A^{\mathrm{eff}} - i\mu\big]\beta_A, \\ \partial_t\beta_A &= -i\big[\Delta_A^{\mathrm{eff}} - i\gamma_A^{\mathrm{eff}}\big]\beta_A - i\big[g_A^{\mathrm{eff}} - i\mu\big]\alpha, \end{aligned} \tag{39}$$

with the same effective parameters as in Eq. (31). Equation (39) describes the effective dynamics for the expectation values of the photon and spin operators a and σ_A^-, respectively, after adiabatic elimination of the degrees of freedom of B. In the Appendix we show that this procedure is generally valid for a situation where the full adiabatic elimination discussed in Sec. III A is valid, i.e., when the eigenvalues of matrix $\mathbf{M}$ (or, equivalently, $\mathbf{B}$) associated with the internal dynamics of B are the largest parameters of the problem. We have thus shown that the time evolution of subsystem $\mathcal{S}$ in the classical limit [Eq. (39)] corresponds to that of the classical fields α and β_A with oscillation frequencies Δ_c^{eff} and Δ_A^{eff} and decay rates κ^{eff} and γ_A^{eff}, respectively, as well as a coupling $\propto g_A^{\mathrm{eff}} - i\mu$ between them.

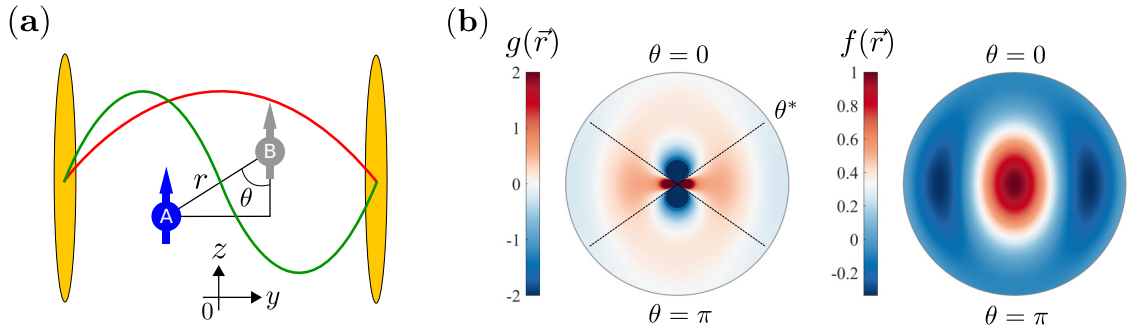

FIG. 2. (a) Two dipoles A and B aligned in the z direction and separated by the vector $\vec{r} = (r, \theta)$ interact via dipole-dipole couplings and with a cavity mode. The first two modes of the cavity are shown as red and green lines. (b) The coherent $[g(\vec{r})]$ and dissipative $[f(\vec{r})]$ dipole-dipole couplings are plotted for polar coordinates (r, θ). The outer circles correspond to $r/\lambda = 1$ (λ: cavity mode wavelength). Since the function $g(\vec{r})$ diverges for $r \to 0$, it is plotted for $g(\vec{r}) \in [-2, 2]$. The thin dashed lines in the $g(\vec{r})$ profile correspond to the magic angles $\theta^* = \arccos(1/\sqrt{3})$ and $\pi - \theta^*$ (see text).

Note that the same classical equations, (39), also follow from the quantum master equation, (27), in the limit of low excitations in $\mathcal{S}$. The fact that the change in the corresponding effective system parameters is identical, in both the full classical and the quantum approach, is interesting. On a qualitative level, the modification of the effective parameters in subsystem $\mathcal{S}$ depends on the dynamics of the B ensemble that it is coupled to. We operate in a regime where the B emitters can be adiabatically eliminated and remain in the low-excitation limit at all times. In this limit the linear classical model for the B ensemble becomes essentially exact. It is thus plausible that the change in the corresponding effective subsystem parameters is the same, independent of whether subsystem $\mathcal{S}$ is treated quantum mechanically or classically. In contrast to the full effective quantum master equation, (27), the classical equations, (39), cannot of course feature quantum correlations between the cavity mode and A since they enforce the factorization $\langle \sigma_A^- a \rangle = \langle \sigma_A^- \rangle \langle a \rangle$. They also cannot lead to nonlinear effects for the photon mode, such as the photon antibunching observed in [20], since the mode is described by a complex number and not an operator. We point out that also in the fully classical derivation of (39) a "correlated" decay at rate μ emerges. We analyze this collective dissipative process in detail in Sec. IV B below.

IV. DISCUSSION OF EFFECTIVE PARAMETERS

In this section we analyze how the physical parameters of subsystem $\mathcal{S}$ [Eq. (31)] are modified and what their limits are, depending on the system parameters and the geometry. Therefore, we consider the case where B is reduced to a single emitter and provide analytical formulas for the effective parameters in this case (Sec. IV A). We find that the presence of B results in a modification of the cavity-coupling strength of A (Sec. IV A 1) and a change in the linewidths (Sec. IV A 2) and leads to joint dissipative processes (Sec. IV A 3). In the second part of this section (Sec. IV B) we analyze the consequences of the joint dissipative processes for the system dynamics. We discuss modifications of cavity transmission spectra (Sec. IV B 1) and modification of the onset of strong cavity coupling of A (Sec. IV B 2).

A. Effective parameters for B being a single emitter

We first consider the situation where B can be considered a single emitter (e.g., a collective mode [20]) at position $\vec{r}_B \equiv (x_B, y_B, z_B)$ separated from A by $\vec{r} \equiv (x, y, z) \equiv \vec{r}_B - \vec{r}_A$ with $\vec{r}_A \equiv (x_A, y_A, z_A)$ [see Fig. 2(a)]. The coupling strength between the A [B] and the cavity mode reads $g_A = g_A^{(0)} \cos(k y_A)$ [$g_B = g_B^{(0)} \cos(k y_B)$]. Here, we choose $g_A^{(0)}, g_B^{(0)} > 0$, and $k = 2\pi/\lambda = \omega_c/c$ denotes the cavity-photon wave vector (along the y direction), with λ the cavity-mode wavelength and c the speed of light in vacuum. We also assume that $k \approx k_A \approx k_B$, with $k_A = \omega_A/c$ and $k_B = \omega_B/c$, which is usually a good approximation at optical frequencies.

The dipole-dipole interaction strength between A and B is [33,34]

$$V_{AB} = -\frac{3\sqrt{\gamma_A \gamma_B}}{2}\left(\sin^2(\theta)\frac{\exp(i\xi)}{\xi} + [3\cos^2(\theta) - 1]\left[\frac{\exp(i\xi)}{\xi^3} - i\frac{\exp(i\xi)}{\xi^2}\right]\right), \tag{40}$$

with $\xi = kr$ ($r \equiv |\vec{r}|$) and $\theta = \arccos(z/r)$. Using $\vec{V} \equiv V_{AB} = \Omega_{AB} - i\gamma_{AB}$, one can compute the quantities $\vec{G}^{\mathrm{T}}\mathbf{M}^{-1}\vec{G}$, $\vec{G}^{\mathrm{T}}\mathbf{M}^{-1}\vec{V}$, and $\vec{V}^{\mathrm{T}}\mathbf{M}^{-1}\vec{V}$ entering Eq. (31), and the effective parameters for the evolution according to Eqs. (27) and (30) become

$$g_A^{\mathrm{eff}} = g_A - g_B\frac{\Omega_{AB}\Delta_B + \gamma_{AB}\gamma_B}{\Delta_B^2 + \gamma_B^2}, \tag{41}$$

$$\gamma_A^{\mathrm{eff}} = \gamma_A + \frac{\gamma_B(\Omega_{AB}^2 - \gamma_{AB}^2) - 2\Delta_B\Omega_{AB}\gamma_{AB}}{\Delta_B^2 + \gamma_B^2}, \tag{42}$$

$$\kappa^{\mathrm{eff}} = \kappa + \frac{g_B^2\gamma_B}{\Delta_B^2 + \gamma_B^2}, \tag{43}$$

$$\mu = g_B\frac{\gamma_B\Omega_{AB} - \Delta_B\gamma_{AB}}{\Delta_B^2 + \gamma_B^2}, \tag{44}$$

and

$$\Delta_A^{\mathrm{eff}} = -\frac{(\Omega_{AB}^2 - \gamma_{AB}^2)\Delta_B + 2\Omega_{AB}\gamma_{AB}\gamma_B}{\Delta_B^2 + \gamma_B^2}, \tag{45}$$

$$\Delta_c^{\mathrm{eff}} = \Delta_c - \frac{g_B^2\Delta_B}{\Delta_B^2 + \gamma_B^2}. \tag{46}$$

The two parameters Δ_B and γ_B are limited by the condition of the validity of the adiabatic elimination, i.e., the effective model. For instance, they have to fulfill

$$\max(|\Omega_{AB}|, |\gamma_{AB}|) \ll |\Delta_B - i\gamma_B|. \tag{47}$$

In the following discussion, we use the two dimensionless functions $g(\vec{r})$ and $f(\vec{r})$, corresponding to the coherent and dissipative parts of the dipole-dipole interaction,

$$\Omega_{AB} = \sqrt{\gamma_A \gamma_B} g(\vec{r}), \tag{48}$$

$$\gamma_{AB} = \sqrt{\gamma_A \gamma_B} f(\vec{r}), \tag{49}$$

respectively. Their geometry dependence is plotted in Fig. 2(b).

1. Effective coupling strength

We first focus on the modification of the coupling strength between A and the cavity mode. Using Eq. (41), the modification of the coupling strength, $\Delta g_A \equiv g_A^{\text{eff}} - g_A$, is

$$\Delta g_A = -g_B \left(\frac{\Omega_{AB}}{|\Delta_B - i\gamma_B|} \frac{\Delta_B}{|\Delta_B - i\gamma_B|} + \frac{\gamma_{AB}}{|\Delta_B - i\gamma_B|} \frac{\gamma_B}{|\Delta_B - i\gamma_B|} \right). \tag{50}$$

Therefore, from Eq. (50) and from Eq. (47) it follows that $|\Delta g_A| \ll |g_B^{(0)}|$, which means that Δg_A generally cannot overcome the cavity-coupling strength of B, as long as the adiabatic elimination condition remains valid.

Using the position dependence of the cavity couplings, the functions $g(\vec{r})$ and $f(\vec{r})$, and the fact that $g_A^{(0)}/g_B^{(0)} = \sqrt{\gamma_A/\gamma_B}$ we can rewrite Eq. (50) as

$$\Delta g_A / g_A^{(0)} = -\cos(k y_B) \frac{\gamma_B}{\Delta_B^2 + \gamma_B^2} \left(\Delta_B g(\vec{r}) + \gamma_B f(\vec{r}) \right). \tag{51}$$

Evidently, the change in the cavity coupling of A can be induced either by coherent [$\propto \Delta_B g(\vec{r})$] or by dissipative [$\propto \gamma_B f(\vec{r})$] dipole-dipole interactions in Eq. (51). Let us now analyze those two limits in more detail.

The dissipative limit $|\gamma_B f(\vec{r})| \gg |\Delta_B g(\vec{r})|$ is difficult to achieve in the near-field, purely by the geometry. This is due to the divergence $|g(\vec{r})| \propto 1/r^3$, while $|f(\vec{r})| \to 1$ for $r \ll \lambda$. An exception is "magic angle" dipole configurations with $3\cos^2(\theta) = 1$, for which near-field terms vanish in Eq. (40), then only implying $|g(\vec{r})| \propto 1/r$ for $r \to 0$ [see Fig. 2(b)]. In general, however, the dissipative limit is achieved for $\Delta_B \approx 0$, i.e., if B is close to resonance with A and the cavity. In this case the validity of the adiabatic elimination in Eq. (47) must be ensured by large γ_B, i.e., by $\gamma_B \gg \gamma_A g^2(\vec{r})$ and $\gamma_B \gg \gamma_A f^2(\vec{r})$. The modification of the cavity coupling becomes

$$\Delta g_A / g_A^{(0)} = -\cos(k y_B) f(\vec{r}). \tag{52}$$

Since $|f(\vec{r})| < 1$, it follows that $|\Delta g_A / g_A^{(0)}| < 1$ and the modification of the coupling strength is therefore generally limited by $g_A^{(0)}$. Still, coherent coupling of A to the cavity can be effectively induced, for instance, when A is at a node of the cavity mode ($g_A = 0$) and B in the near-field of A with $r \ll \lambda$ and $\cos(k y_B) \neq 0$ [20].

The coherent limit $|\Delta_B g(\vec{r})| \gg |\gamma_B f(\vec{r})|$ is generally achieved for most configurations in the near-field where $|g(\vec{r})| \gg |f(\vec{r})|$, as long as $|\Delta_B| \gtrsim \gamma_B$. The modification of the coupling,

$$\Delta g_A / g_A^{(0)} = -\cos(k y_B) g(\vec{r}) \frac{\Delta_B \gamma_B}{\Delta_B^2 + \gamma_B^2}, \tag{53}$$

is then generally limited by the magnitude of $g(\vec{r})$. In a regime where the adiabatic elimination condition, (47), is valid, if $|\Delta_B| \sim \gamma_B$, it is required that $|\Omega_{AB}| \ll \gamma_B$ and thus $|g(\vec{r})| \ll \sqrt{\gamma_B/\gamma_A}$. On the other hand, condition (47) can be easily fulfilled for large detuning, $|\Delta_B| \gg \gamma_B$, in this case

$$\Delta g_A / g_A^{(0)} = -\cos(k y_B) g(\vec{r}) \frac{\gamma_B}{\Delta_B} \ll |g(\vec{r})|. \tag{54}$$

While the change in coupling strength is still limited by $|g(\vec{r})|$, generally large enhancements of g_A are possible in this regime [20].

2. Effective linewidths

We now focus on the linewidth modifications of the cavity and A. From Eq. (43), it is evident that the cavity mode linewidth κ can only be broadened by the interaction with B since

$$\Delta\kappa \equiv \kappa^{\text{eff}} - \kappa = \frac{g_B^2 \gamma_B}{\Delta_B^2 + \gamma_B^2} \geqslant 0. \tag{55}$$

The change in effective linewidth of A, $\Delta\gamma_A \equiv \gamma_A^{\text{eff}} - \gamma_A$, using Eq. (42), can be written in the form

$$\Delta\gamma_A / \gamma_A = \left[\frac{[\gamma_B g(\vec{r}) - \Delta_B f(\vec{r})]^2}{\Delta_B^2 + \gamma_B^2} - f^2(\vec{r}) \right]. \tag{56}$$

The first term in Eq. (56),

$$\frac{[\gamma_B g(\vec{r}) - \Delta_B f(\vec{r})]^2}{\Delta_B^2 + \gamma_B^2} \geqslant 0, \tag{57}$$

always leads to a broadening of γ_A, while the second term, $f^2(\vec{r}) \geqslant 0$, always contributes to a linewidth reduction.

Importantly, strong linewidth narrowing is possible for special points for which the broadening from Eq. (57) vanishes, i.e., when

$$\gamma_B g(\vec{r}) = \Delta_B f(\vec{r}) \tag{58}$$

is fulfilled. Then one can achieve large linewidth reductions $\Delta\gamma_A/\gamma_A \to -1$ in the near-field, where $f(\vec{r}) \to 1$. Furthermore, we note that a reduction can also be achieved in the dissipative limit with $\Delta_B = 0$, discussed above. Then

$$\Delta\gamma_A / \gamma_A = \left[g^2(\vec{r}) - f^2(\vec{r}) \right], \tag{59}$$

and $\gamma_A^{\text{eff}} < \gamma_A$ occurs for any geometry with $|f(\vec{r})| > |g(\vec{r})|$, e.g., close to the magic angle $\theta^* = \arccos(1/\sqrt{3})$ in the near-field [see Fig. 2(b)].

3. Joint dissipative couplings

We now focus on the effective parameter μ that enters as a collective dissipative term in Eq. (30). Defining the (positive)

broadening of A as

$$\delta\gamma_A \equiv \gamma_A \frac{[\gamma_B g(\vec{r}) - \Delta_B f(\vec{r})]^2}{\Delta_B^2 + \gamma_B^2}, \tag{60}$$

the modulus of μ [Eq. (44)] can be written in the very simple form

$$|\mu| = \sqrt{\Delta\kappa\,\delta\gamma_A}. \tag{61}$$

Since $\delta\gamma_A < \gamma_A^{\rm eff}$ and $\Delta\kappa < \kappa^{\rm eff}$, this implies that $|\mu| < \sqrt{\kappa^{\rm eff}\gamma_A^{\rm eff}} \leqslant \max(\kappa^{\rm eff}, \gamma_A^{\rm eff})$, which sets a fundamental limitation on $|\mu|$. Note that at special points of ideal linewidth narrowing [condition (58)], $\delta\gamma_A = 0$ and then also $\mu = 0$.

B. Consequences of joint dissipative coupling

Importantly, the new dissipative terms in Eq. (30) are not in Lindblad form, i.e., they do not consist only of terms $\mathcal{D}(L^\dagger, L)$, with L a Lindblad operator. In addition to the "diagonal" decay of the cavity $[\mathcal{D}(a^\dagger, a)]$ and A $[\mathcal{D}(\sigma_A^+, \sigma_A^-)]$, there are also off-diagonal decay processes involving both the cavity and A $[\mathcal{D}(a^\dagger, \sigma_A^-)$ and $\mathcal{D}(\sigma_A^+, a)]$, which are not present in the bare system decay in Eq. (5). To bring Eq. (30) back into a Lindblad form, we define new collective operators

$$L_+ = \cos(\alpha/2)a + \sin(\alpha/2)\sigma_A^-, \tag{62}$$

$$L_- = -\sin(\alpha/2)a + \cos(\alpha/2)\sigma_A^-. \tag{63}$$

Then Eq. (30) can be written as

$$\mathcal{L}^{\rm eff} v = -\gamma_+ \mathcal{D}(L_+^\dagger, L_+)v - \gamma_- \mathcal{D}(L_-^\dagger, L_-)v. \tag{64}$$

The Lindblad operators are linear combinations of the photon annihilation operator a and the spin-lowering operator σ_A^-, with $\tan(\alpha) = 2\mu/(\kappa^{\rm eff} - \gamma_A^{\rm eff})$ and $0 \leqslant \alpha < 2\pi$. The decay rates associated with the Lindblad operators are

$$\gamma_\pm = \frac{\kappa^{\rm eff} + \gamma_A^{\rm eff}}{2} \pm \sqrt{\frac{(\kappa^{\rm eff} - \gamma_A^{\rm eff})^2}{4} + \mu^2} \tag{65}$$

and correspond to the eigenvalues of the matrix

$$\begin{pmatrix} \kappa^{\rm eff} & \mu \\ \mu & \gamma_A^{\rm eff} \end{pmatrix}. \tag{66}$$

The two Lindblad jump operators describe mutual decay processes between the cavity and A, which are mediated by the presence of B. This is analogous to sub- and superradiant decay of atoms due to collective incoherent processes, induced by the coupling to a joint cavity mode [36,46]. Similarly, also the parameters γ_{jA} introduced in Sec. II correspond to such off-diagonal decay mechanisms, which are in this case mediated by the surrounding electromagnetic field [33].

In the following, we now investigate the consequences of the mutual decay mechanisms between the cavity mode and A in the effective model that is mediated by the presence of ensemble B. We analyze the modification of the cavity transmission spectum in Sec. IV B 1 and study the modification of the onset of strong coupling between the cavity and A in Sec. IV B 2.

1. Cavity transmission spectrum

To compute a cavity transmission spectrum, we consider a weak laser probe driving the cavity, described by the (additional) time-dependent Hamiltonian

$$H_L = \eta(a e^{i\omega_L t} + a^\dagger e^{-i\omega_L t}) \tag{67}$$

with frequency ω_L and strength η.

Similarly as in Sec. III B, we derive the equations of motion in the classical linear limit valid for low excitation numbers (initial state without excitations and weak drive $\eta \to 0$). Then, using the classical variables $\alpha \equiv \langle a\rangle$, $\beta_A \equiv \langle\sigma_A^-\rangle$, and $\vec{\beta} \equiv \langle\vec{\sigma}_-\rangle$, in the frame rotating with the laser frequency ω_L, the equations of motion are

$$\partial_t\alpha = -i[\widetilde{\Delta}_c - i\kappa]\alpha - ig_A\beta_A - i\vec{G}^{\rm T}\vec{\beta} - i\eta, \tag{68}$$

$$\partial_t\beta_A = -i\big[\widetilde{\Delta}_A - i\gamma_A\big]\beta_A - ig_A\alpha - i\vec{V}^{\rm T}\vec{\beta}, \tag{69}$$

$$\partial_t\vec{\beta} = -i\widetilde{\mathbf{M}}\vec{\beta} - i\vec{G}\alpha - i\vec{V}\beta_A, \tag{70}$$

where $\widetilde{\Delta}_c = \omega_c - \omega_L$, $\widetilde{\Delta}_A = \omega_A - \omega_L$, and $(\widetilde{\mathbf{M}})_{j\ell} = (\widetilde{\Delta}_B - i\gamma_B)\delta_{j\ell} + (1 - \delta_{j\ell})(\Omega_{j\ell} - i\gamma_{j\ell})$ with $\widetilde{\Delta}_B = \omega_B - \omega_L$. The steady-state solution is

$$\begin{pmatrix} \alpha^{\rm st} \\ \beta_A^{\rm st} \end{pmatrix} = -\begin{pmatrix} \widetilde{\Delta}_c^{\rm eff} - i\widetilde{\kappa}^{\rm eff} & \widetilde{g}_A^{\rm eff} - i\widetilde{\mu} \\ \widetilde{g}_A^{\rm eff} - i\widetilde{\mu} & \widetilde{\Delta}_A^{\rm eff} - i\widetilde{\gamma}_A^{\rm eff} \end{pmatrix}^{-1} \begin{pmatrix} \eta \\ 0 \end{pmatrix}, \tag{71}$$

with the definitions

$$\begin{aligned} \widetilde{\Delta}_c^{\rm eff} &= \widetilde{\Delta}_c - {\rm Re}[\vec{G}^{\rm T}\widetilde{\mathbf{M}}^{-1}\vec{G}], & \widetilde{\Delta}_A^{\rm eff} &= \widetilde{\Delta}_A - {\rm Re}[\vec{V}^{\rm T}\widetilde{\mathbf{M}}^{-1}\vec{V}], \\ \widetilde{g}_A^{\rm eff} &= g_A - {\rm Re}[\vec{G}^{\rm T}\widetilde{\mathbf{M}}^{-1}\vec{V}], & \widetilde{\kappa}^{\rm eff} &= \kappa + {\rm Im}[\vec{G}^{\rm T}\widetilde{\mathbf{M}}^{-1}\vec{G}], \\ \widetilde{\gamma}_A^{\rm eff} &= \gamma_A + {\rm Im}[\vec{V}^{\rm T}\widetilde{\mathbf{M}}^{-1}\vec{V}], & \widetilde{\mu} &= {\rm Im}[\vec{G}^{\rm T}\widetilde{\mathbf{M}}^{-1}\vec{V}]. \end{aligned} \tag{72}$$

The cavity transmission spectrum is proportional to the mean photon number in the steady state $\propto |\alpha^{\rm st}|^2$, which can be obtained from Eq. (71).

We consider a situation where the eigenvalues of the matrix in the laser frame, $\widetilde{\mathbf{M}} = \mathbf{M} + \mathbb{1}(\omega_A - \omega_L)$ ($\mathbb{1}$ is the identity matrix), are well approximated by the eigenvalues of $\mathbf{M}$. This is true when the shift $|\omega_A - \omega_L|$ is small compared to the real part of the eigenvalues of $\mathbf{M}$, which are related to the eigenfrequencies of the interacting B ensemble. Note that this condition can be ensured in the dispersive limit (where the eigenfrequencies of B are far detuned, i.e., spectrally well separated from $\mathcal{S}$) and that this is consistent with the requirement for the validity of the adiabatic elimination (see the Appendix), also in the presence of the laser drive. The probe laser is then scanned only over a frequency range that is relevant for the dynamics of the subsystem $\mathcal{S}$. In this situation $\widetilde{\kappa}^{\rm eff} \approx \kappa^{\rm eff}$, $\widetilde{\gamma}_A^{\rm eff} \approx \gamma_A^{\rm eff}$, $\widetilde{g}_A^{\rm eff} \approx g_A^{\rm eff}$, $\widetilde{\mu} \approx \mu$, and the laser frequency only enters through the detunings $\widetilde{\Delta}_c^{\rm eff} = \omega_c^{\rm eff} - \omega_L$ and $\widetilde{\Delta}_A^{\rm eff} = \omega_A^{\rm eff} - \omega_L$ with $\omega_c^{\rm eff} \simeq \omega_c - {\rm Re}[\vec{G}^{\rm T}\mathbf{M}^{-1}\vec{G}]$ and $\omega_A^{\rm eff} \simeq \omega_A - {\rm Re}[\vec{V}^{\rm T}\mathbf{M}^{-1}\vec{V}]$. Then we define the normalized steady-state cavity transmission spectrum by $\mathcal{T}_c(\omega_L) \equiv (\kappa^2/\eta^2)|\alpha^{\rm st}|^2$ with

$$\alpha^{\rm st} = \frac{\eta\big(\widetilde{\Delta}_A^{\rm eff} - i\gamma_A^{\rm eff}\big)}{\big(g_A^{\rm eff} - i\mu\big)^2 - \big(\widetilde{\Delta}_A^{\rm eff} - i\gamma_A^{\rm eff}\big)\big(\widetilde{\Delta}_c^{\rm eff} - i\kappa^{\rm eff}\big)}. \tag{73}$$

For a finite mutual decay rate $\mu \neq 0$, we find that this transmission spectrum features two asymmetric peaks sepa-

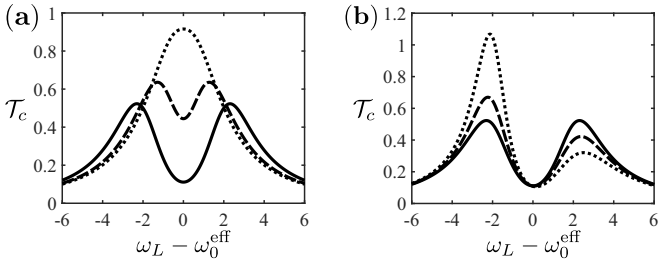

FIG. 3. Normalized steady-state cavity transmission spectra $\mathcal{T}_c$. (a) $\mu = 0$: Dotted, dashed, and solid lines correspond to $g_A^{\rm eff} = 0.3$, 1, and 2, respectively. (b) $g_A^{\rm eff} = 2$: Solid, dashed, and dotted lines correspond to $\mu = 0$, 0.2, and 0.5, respectively. All parameters are in units of $g_A^{(0)} \equiv 1$. Here, $\gamma_A^{\rm eff} = 1$, $\kappa^{\rm eff} = 2$, and $\eta = 0.1$.

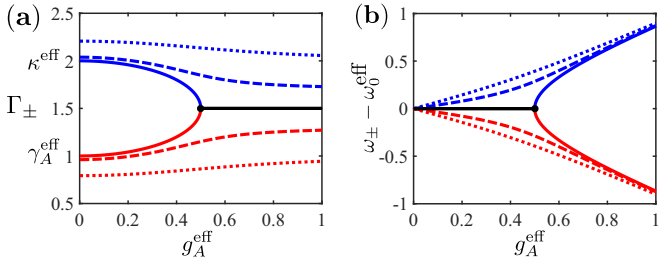

FIG. 4. Polariton linewidths $\Gamma_\pm$ (a) and frequencies $\omega_\pm$ (b) as a function of $g_A^{\rm eff} \geqslant 0$ for different $\mu \geqslant 0$. The upper (here ξ_+) and lower (here ξ_-) polaritons are depicted as blue and red lines, while the solid, dashed, and dotted lines correspond to $\mu = 0$, 0.2, and 0.5, respectively. All parameters are in units of $g_A^{(0)} \equiv 1$. Here, $\gamma_A^{\rm eff} = 1$ and $\kappa^{\rm eff} = 2$.

rated by an energy splitting $\propto 2|g_A^{\rm eff}|$ for large enough $g_A^{\rm eff}$. It is instructive to associate the peaks with "polaritons" by diagonalizing the matrix entering Eq. (71). Considering A in resonance with the cavity mode, i.e., $\omega_A^{\rm eff} = \omega_c^{\rm eff} \equiv \omega_0^{\rm eff}$, and by defining $\widetilde{\Delta}^{\rm eff} = \omega_0^{\rm eff} - \omega_L$, Eq. (71) can be decomposed as (assuming the dispersive limit)

$$\begin{pmatrix} \alpha^{\rm st} \\ \\ \beta_A^{\rm st} \end{pmatrix} = \left\{ -i\mathbf{T} - \begin{pmatrix} \widetilde{\Delta}^{\rm eff} & 0 \\ \\ 0 & \widetilde{\Delta}^{\rm eff} \end{pmatrix} \right\}^{-1} \begin{pmatrix} \eta \\ \\ 0 \end{pmatrix}, \tag{74}$$

where

$$\mathbf{T} = \begin{pmatrix} -\kappa^{\rm eff} & -ig_A^{\rm eff} - \mu \\ \\ -ig_A^{\rm eff} - \mu & -\gamma_A^{\rm eff} \end{pmatrix} \tag{75}$$

is a non-Hermitian, complex symmetric matrix, which we diagonalize as $\mathbf{T} = \sum_{p=\pm} \xi_p \vec{u}_p \vec{u}_p^{\rm T}$. Here, the two eigenvectors are defined as $\vec{u}_+ = (u_1^+, u_2^+)$ and $\vec{u}_- = (u_1^-, u_2^-)$, with $\sum_{p=\pm} \vec{u}_p \vec{u}_p^{\rm T} = \mathbb{1}$. The eigenvalues are

$$\xi_\pm = -\frac{\gamma_A^{\rm eff} + \kappa^{\rm eff}}{2} \mp \sqrt{\left(\frac{\kappa^{\rm eff} - \gamma_A^{\rm eff}}{2}\right)^2 - \left(g_A^{\rm eff} - i\mu\right)^2}. \tag{76}$$

We introduce the polariton linewidths and frequencies associated with the real and imaginary parts of $\xi_\pm$, namely, $\Gamma_\pm = -{\rm Re}[\xi_\pm]$ and $\omega_\pm = \omega_0^{\rm eff} - {\rm Im}[\xi_\pm]$. This leads to

$$\mathcal{T}_c(\omega_L) = \kappa^2 \left| \frac{Z_+}{\omega_L - \omega_+ + i\Gamma_+} + \frac{Z_-}{\omega_L - \omega_- + i\Gamma_-} \right|^2, \tag{77}$$

where $Z_+ = u_1^+ u_2^- / (u_1^+ u_2^- - u_1^- u_2^+)$ and $Z_- = u_1^- u_2^+ / (u_1^- u_2^+ - u_1^+ u_2^-)$ are related to the cavity and spin admixtures of the polaritons eigenmodes.

Cavity transmission spectra from Eq. (77) are plotted for $\mu = 0$ and different effective coupling strengths $g_A^{\rm eff}$ in Fig. 3(a) and for $g_A^{\rm eff} = 2$ and different mutual decay rates μ in Fig. 3(b). For $\mu = 0$, the spectrum is symmetric with respect to $\omega_0^{\rm eff}$, and increasing $g_A^{\rm eff}$ allows it to enter the strong-coupling regime characterized by the emergence of two well-resolved polariton peaks. We find that increasing $\mu > 0$ leads to an asymmetric spectrum with two peaks of different heights and linewidths $\Gamma_+ > \Gamma_-$, which is a common feature discussed for cavity-coupled molecules [47–49]. In particular, we find that here the joint dissipative processes between A and the cavity lead to a lower or upper polariton with a subradiant or superradiant linewidth, respectively.

2. *Onset of strong coupling*

Finally, we focus on how a finite $\mu \neq 0$ modifies the conditions for reaching strong coupling between A and the cavity. The polariton linewidths $\Gamma_\pm$ and frequencies $\omega_\pm$ are plotted in Figs. 4(a) and 4(b), respectively, as a function of $g_A^{\rm eff} \geqslant 0$ for different $\mu \geqslant 0$.

We first focus on the case $\mu = 0$ (solid lines). For $g_A^{\rm eff} < |\kappa^{\rm eff} - \gamma_A^{\rm eff}|/2$, the two polariton modes are undefined, and the eigenmodes of the system have frequencies $\omega_\pm = \omega_0^{\rm eff}$ and linewidths $\Gamma_\pm$ with $\min(\gamma_A^{\rm eff}, \kappa^{\rm eff}) \leqslant \Gamma_- \leqslant \Gamma_+ \leqslant \max(\gamma_A^{\rm eff}, \kappa^{\rm eff})$. In this weak-coupling regime, the cavity transmission spectrum features two strongly overlapping peaks [see Fig. 3(a)], and the time evolution of the system exhibits overdamped Rabi oscillations.

For $\mu = 0$, the strong coupling is reached when $g_A^{\rm eff} > |\kappa^{\rm eff} - \gamma_A^{\rm eff}|/2$ or, alternatively, when $g_A^{\rm eff} > \max(\gamma_A^{\rm eff}, \kappa^{\rm eff})$. In this case, two polariton modes with different frequencies, $\omega_\pm$, and identical linewidths, $(\kappa^{\rm eff} + \gamma_A^{\rm eff})/2$, emerge. The transmission spectrum features two weakly overlapping peaks [see Fig. 3(a)], and the dynamics of $\mathcal{S}$ exhibits well-defined Rabi oscillations. The two eigenvalues $\xi_\pm$ coalesce for the "exceptional point" $g_A^{\rm eff} = (\kappa^{\rm eff} - \gamma_A^{\rm eff})/2$ [50,51].

Finite $\mu \neq 0$ affects the onset of strong coupling. In this case, the degeneracy of the two eigenvalues $\xi_\pm$ is removed and the exceptional point for the onset of strong coupling disappears. The polariton linewidths and frequencies are different for all $g_A^{\rm eff}$. By calculating the first derivative of the linewidth Γ_+ with respect to $g_A^{\rm eff} \geqslant 0$, we find that Γ_+ is a monotonically decreasing function of $g_A^{\rm eff}$. Therefore, the most restrictive condition for strong coupling in the case $\mu \neq 0$ is $g_A^{\rm eff} > \gamma_+$, where

$$\gamma_+ \equiv \Gamma_+(g_A^{\rm eff} = 0) = \frac{\gamma_A^{\rm eff} + \kappa^{\rm eff}}{2} + \sqrt{\left(\frac{\kappa^{\rm eff} - \gamma_A^{\rm eff}}{2}\right)^2 + \mu^2}. \tag{78}$$

We note that for the discussion of Fig. 3 and Fig. 4 above, $\mu \geqslant 0$ and $g_A^{\rm eff} \geqslant 0$ have been assumed. The fact that the lower and upper polaritons display subradiant and superradiant properties, respectively, is a consequence of this. The

features presented in Figs. 3 and 4 hold for arbitrary μ and $g_A^{\rm eff}$, whereas for $\mu g_A^{\rm eff} < 0$ the asymmetry is reversed, i.e., the lower (upper) polariton exhibits superradiant (subradiant) behavior.

V. CONCLUSION AND OUTLOOK

In conclusion, we have carried out a detailed study of the impact of a dipolar environment on the dynamics of a single dipole A coupled to a cavity mode. We performed a detailed adiabatic elimination of the dipoles in the environment and computed effective parameters for the subsystem consisting of A and the cavity. Since the dipoles in the environment couple to both A (with full coherent and dissipative dipole-dipole interactions) and the cavity, they modify the properties of the subsystem significantly. We analyzed effective modifications and limitations of subsystem linewidths, coherent cavity-coupling strengths, and emerging collective dissipative processes between A and the cavity. In particular, the latter joint dissipative decay processes can lead to peculiar signatures in the strong-coupling regime.

Our work highlights the impact of "active" environments on cavity-QED systems, which are relevant in the field of molecular polaritonics [11,17,52–55] where environments such as solvents can play a crucial role [18,19]. There, other interesting perspectives of this work include extensions to disordered ensembles in the context of the emergent field of polaritonic chemistry.

ACKNOWLEDGMENTS

We are grateful to C. Genes for stimulating discussions and appreciate helpful comments by G. Morigi. This work was supported by the ANR, ERA-NET QuantERA, Project RouTe (ANR-18-QUAN-0005-01), and LabEx NIE (Nanostructures in Interaction with their Environment) under contract ANR-11-LABX-0058_NIE within the Investissement d'Avenir program ANR-10-IDEX-0002-02. G.P. acknowledges support from the Institut Universitaire de France (IUF) and the University of Strasbourg Institute of Advanced Studies (USIAS). Research was carried out using computational resources of the Centre de calcul de l'Université de Strasbourg.

APPENDIX: VALIDITY OF THE ADIABATIC APPROXIMATION

In this Appendix, we discuss in more detail the conditions required for the validity of the adiabatic elimination of B, using the derivation of the model in the classical limit (Sec. III B). We derive the general condition, under which the steady-state solution for the B ensemble [Eq. (38)] can be inserted into Eqs. (35) and (36) to obtain the set of equations in (39).

We first write Eq. (37) as $\partial_t \vec{\beta} = \mathbf{B}\vec{\beta}(t) + \vec{S}(t)$ with $\mathbf{B} = -i\mathbf{M}$ and $\vec{S}(t) = -i[\vec{G}\alpha(t) + \vec{V}\beta_A(t)]$. The formal solution of this differential equation reads $\vec{\beta}(t) = e^{\mathbf{B}t}\vec{\beta}(0) + \int_0^t d\tau' e^{\mathbf{B}\tau'}\vec{S}(t-\tau')$. The eigenvalues of matrix $\mathbf{B}$ are given by λ_j (as in Sec. III A 4). These eigenvalues determine the fast dynamics of the interacting B ensemble. For simplicity, we assume the limit of large t (with $\mathrm{Re}\{\lambda_j\} < 0$) and set the upper limit of integration to infinity,

$$\vec{\beta}(t) = \int_0^\infty d\tau' e^{\mathbf{B}\tau'}\vec{S}(t-\tau'). \tag{A1}$$

The first term $e^{\mathbf{B}t}\vec{\beta}(0)$ vanishes when assuming the initial condition $\vec{\beta}(0) = 0$ similarly as in Sec. III A. If the ensemble emitters are initially (here $t = 0$) sufficiently close to the ground state, the first term $e^{\mathbf{B}t}\vec{\beta}(0)$ becomes negligible when one averages over a time interval $\Delta t \gg |\lambda_j|^{-1}$, where Δt is a coarse-grained time scale assumed to be large compared to the typical time scale associated with the dynamics of the B ensemble but small compared to the time scale of the effective dynamics of subsystem $\mathcal{S}$. In other words, this requires a time-scale separation between the B ensemble and subsystem $\mathcal{S}$.

Using the definition $\mathbf{B} = \sum_j \lambda_j \vec{x}_j \vec{x}_j^{\rm T}$ from Sec. III A 4, Eq. (A1) provides $\vec{\beta}(t) = \sum_j \vec{x}_j \int_0^\infty d\tau' e^{\lambda_j \tau'} \vec{x}_j^{\rm T}\vec{S}(t-\tau')$. After integration by parts, the previous equation can be written as $\vec{\beta}(t) = \vec{\beta}_{\rm ad}(t) + \vec{\beta}_{\rm ret}(t)$ with

$$\vec{\beta}_{\rm ad}(t) = -\sum_j \frac{\vec{x}_j}{\lambda_j}\vec{x}_j^{\rm T}\vec{S}(t) = i\sum_j \frac{\vec{x}_j}{\lambda_j}\left[\vec{x}_j^{\rm T}\vec{G}\alpha(t) + \vec{x}_j^{\rm T}\vec{V}\beta_A(t)\right], \tag{A2}$$

$$\vec{\beta}_{\rm ret}(t) = -\sum_j \frac{\vec{x}_j}{\lambda_j}\int_0^\infty d\tau' e^{\lambda_j\tau'}\partial_{\tau'}\vec{x}_j^{\rm T}\vec{S}(t-\tau'). \tag{A3}$$

Using the relation $\mathbf{B}^{-1} = i\mathbf{M}^{-1} = \sum_j \vec{x}_j\vec{x}_j^{\rm T}/\lambda_j$, one can write the *adiabatic solution* $\vec{\beta}_{\rm ad}(t)$ in Eq. (A2) in the form of Eq. (38), namely, $\vec{\beta}_{\rm ad}(t) = -\mathbf{M}^{-1}\vec{G}\alpha(t) - \mathbf{M}^{-1}\vec{V}\beta_A(t)$. Furthermore, since $\alpha(t)$ and $\beta_A(t)$ are, respectively, of order $\sqrt{\bar{n}}$ (with $\bar{n}$ the mean photon number) and unity, the condition $|\vec{\beta}(t)|^2 \ll 1$ of low population for spins B requires $|\vec{x}_j^{\rm T}\vec{V}| \ll |\lambda_j|$ and $|\vec{x}_j^{\rm T}\vec{G}|\sqrt{\bar{n}} \ll |\lambda_j|$. In the limit of small $\bar{n}$ (vacuum-Rabi couplings), the latter requirement reads $|\vec{x}_j^{\rm T}\vec{G}| \ll |\lambda_j|$. The previous conditions are consistent with assuming a sufficiently weak coupling between the B ensemble and subsystem $\mathcal{S}$, which justifies a perturbative treatment of the interaction (as in Sec. III).

The solution $\vec{\beta}_{\rm ret}(t)$ [Eq. (A3)] is associated with retardation effects and was neglected in Eq. (38) provided $\vec{\beta}_{\rm ret}(t) \ll \vec{\beta}_{\rm ad}(t)$. In order to justify this approximation, we now estimate the contribution $\vec{\beta}_{\rm ret}(t)$ in a self-consistent manner, which allows us to obtain the leading-order correction to the adiabatic solution. We start from Eq. (A3) with the definition of $\vec{S}(t)$ and calculate the time derivatives $\partial_{\tau'}\alpha(t-\tau')$ and $\partial_{\tau'}\beta_A(t-\tau')$ using Eqs. (35) and (36). This leads to

$$\vec{\beta}_{\rm ret}(t) = -\sum_j \frac{\vec{x}_j}{\lambda_j}\int_0^\infty d\tau' e^{\lambda_j\tau'}\Big\{\vec{x}_j^{\rm T}\vec{G}\Big[(\Delta_c - i\kappa)\alpha(t-\tau') + g_A\beta_A(t-\tau') + \vec{G}^{\rm T}\vec{\beta}(t-\tau')\Big] + \vec{x}_j^{\rm T}\vec{V}\Big[-i\gamma_A\beta_A(t-\tau') + g_A\alpha(t-\tau') + \vec{V}^{\rm T}\vec{\beta}(t-\tau')\Big]\Big\}. \tag{A4}$$

Now replacing $\vec{\beta}(t-\tau')$ with its adiabatic solution $\vec{\beta}(t-\tau') \approx \vec{\beta}_{\rm ad}(t-\tau')$, the term $\vec{\beta}_{\rm ret}(t)$ is estimated as

$$\vec{\beta}_{\rm ret}(t) \approx -\sum_j \frac{\vec{x}_j}{\lambda_j}\int_0^\infty d\tau' e^{\lambda_j\tau'}\Big\{\vec{x}_j^{\rm T}\vec{G}\Big[(\Delta_c - i\kappa)\alpha(t) + g_A\beta_A(t) + \vec{G}^{\rm T}\Big(-\mathbf{M}^{-1}\vec{G}\alpha(t) - \mathbf{M}^{-1}\vec{V}\beta_A(t)\Big)\Big] + \vec{x}_j^{\rm T}\vec{V}\Big[-i\gamma_A\beta_A(t) + g_A\alpha(t) + \vec{V}^{\rm T}\Big(-\mathbf{M}^{-1}\vec{G}\alpha(t) - \mathbf{M}^{-1}\vec{V}\beta_A(t)\Big)\Big]\Big\}. \tag{A5}$$

Here, we have also replaced $\alpha(t-\tau')$ with $\alpha(t)$ and $\beta_A(t-\tau')$ with $\beta_A(t)$ in the integrand, similarly to the approximations $\rho_{gg}(t-\tau) \approx \rho_{gg}(t)$ and $\exp[(\mathcal{L}_B + \mathcal{L}_S)\tau] \approx \exp[\mathcal{L}_B\tau]$ in Sec. III A, which hold when the time scales associated with the dynamics of B and subsystem $\mathcal{S}$ are well separated. Using the definitions of the effective parameters in Eq. (31), the retarded solution reads

$$\vec{\beta}_{\rm ret}(t) \approx \sum_j \frac{\vec{x}_j}{\lambda_j^2}\Big\{\vec{x}_j^{\rm T}\vec{G}\big[\big(\Delta_c^{\rm eff} - i\kappa^{\rm eff}\big)\alpha(t) + \big(g_A^{\rm eff} - i\mu\big)\beta_A(t)\big] + \vec{x}_j^{\rm T}\vec{V}\big[\big(\Delta_A^{\rm eff} - i\gamma_A^{\rm eff}\big)\beta_A(t) + \big(g_A^{\rm eff} - i\mu\big)\alpha(t)\big]\Big\}. \tag{A6}$$

By comparing Eqs. (A2) and (A6), we find that $|\Delta_c^{\rm eff} - i\kappa^{\rm eff}| \ll |\lambda_j|$, $|\Delta_A^{\rm eff} - i\gamma_A^{\rm eff}| \ll |\lambda_j|$, and $\sqrt{\bar{n}}|g_A^{\rm eff} - i\mu| \ll |\lambda_j|$ are necessary conditions to neglect retardation effects ($\vec{\beta}_{\rm ret} \ll \vec{\beta}_{\rm ad}$). These conditions correspond to a separation of the different time scales, namely, that the dynamics of subsystem $\mathcal{S}$ is slow compared to that of B, consistent with the substitutions $\alpha(t-\tau') \approx \alpha(t)$ and $\beta_A(t-\tau') \approx \beta_A(t)$.

In conclusion, the global condition for adiabatic elimination of B is that λ_j are the largest parameters of the problem, in agreement with the arguments in Sec. III used in the derivation of the effective master equation. Note that when B is reduced to a single spin, this condition becomes $|\Delta_B - i\gamma_B| \gg \{|\Omega_{AB} - i\gamma_{AB}|, |g_B|\sqrt{\bar{n}}, |\Delta_c^{\rm eff} - i\kappa^{\rm eff}|, |\Delta_A^{\rm eff} - i\gamma_A^{\rm eff}|, \sqrt{\bar{n}}|g_A^{\rm eff} - i\mu|\}$.

[1] E. T. Jaynes and F. W. Cummings, Proc. IEEE **51**, 89 (1963).
[2] H. J. Kimble, Phys. Scr. **T76**, 127 (1998).
[3] J. M. Raimond, M. Brune, and S. Haroche, Rev. Mod. Phys. **73**, 565 (2001).
[4] Y. Kaluzny, P. Goy, M. Gross, J. M. Raimond, and S. Haroche, Phys. Rev. Lett. **51**, 1175 (1983).
[5] M. G. Raizen, R. J. Thompson, R. J. Brecha, H. J. Kimble, and H. J. Carmichael, Phys. Rev. Lett. **63**, 240 (1989).
[6] R. J. Thompson, G. Rempe, and H. J. Kimble, Phys. Rev. Lett. **68**, 1132 (1992).
[7] A. Imamoğlu, R. J. Ram, S. Pau, and Y. Yamamoto, Phys. Rev. A **53**, 4250 (1996).
[8] H. Deng, G. Weihs, C. Santori, J. Bloch, and Y. Yamamoto, Science **298**, 199 (2002).
[9] J. Kasprzak, M. Richard, S. Kundermann, A. Baas, P. Jeambrun, J. M. J. Keeling, F. M. Marchetti, M. H. Szymańska, R. André, J. L. Staehli, V. Savona, P. B. Littlewood, B. Deveaud, and L. S. Dang, Nature **443**, 409 (2006).
[10] A. Amo, J. Lefrère, S. Pigeon, C. Adrados, C. Ciuti, I. Carusotto, R. Houdré, E. Giacobino, and A. Bramati, Nat. Phys. **5**, 805 (2009).
[11] J. A. Hutchison, T. Schwartz, C. Genet, E. Devaux, and T. W. Ebbesen, Angew. Chem. **51**, 1592 (2012).
[12] D. M. Coles, N. Somaschi, P. Michetti, C. Clark, P. G. Lagoudakis, P. G. Savvidis, and D. G. Lidzey, Nat. Mater. **13**, 712 (2014).
[13] E. Orgiu, J. George, J. A. Hutchison, E. Devaux, J. F. Dayen, B. Doudin, F. Stellacci, C. Genet, J. Schachenmayer, C. Genes, G. Pupillo, P. Samorì, and T. W. Ebbesen, Nat. Mater. **14**, 1123 (2015).
[14] J. Galego, F. J. Garcia-Vidal, and J. Feist, Nat. Commun. **7**, 13841 (2016).
[15] X. Zhong, T. Chervy, L. Zhang, A. Thomas, J. George, C. Genet, J. A. Hutchison, and T. W. Ebbesen, Angew. Chem. Int. Ed. **56**, 9034 (2017).
[16] M. A. Sentef, M. Ruggenthaler, and A. Rubio, Sci. Adv. **4**, eaau6969 (2018).
[17] A. Thomas, L. Lethuillier-Karl, K. Nagarajan, R. M. A. Vergauwe, J. George, T. Chervy, A. Shalabney, E. Devaux, C. Genet, J. Moran, and T. W. Ebbesen, Science **363**, 615 (2019).
[18] J. Lather, P. Bhatt, A. Thomas, T. W. Ebbesen, and J. George, Angew. Chem. Int. Ed. **58**, 10635 (2019).
[19] A. Thomas, E. Devaux, K. Nagarajan, T. Chervy, M. Seidel, D. Hagenmüller, S. Schütz, J. Schachenmayer, C. Genet, G. Pupillo, and T. W. Ebbesen, arXiv:1911.01459.
[20] S. Schütz, J. Schachenmayer, D. Hagenmüller, G. K. Brennen, T. Volz, V. Sandoghdar, T. W. Ebbesen, C. Genes, and G. Pupillo, Phys. Rev. Lett. **124**, 113602 (2020).
[21] G. Rempe, R. J. Thompson, R. J. Brecha, W. D. Lee, and H. J. Kimble, Phys. Rev. Lett. **67**, 1727 (1991).
[22] H. J. Carmichael, R. J. Brecha, and P. R. Rice, Opt. Commun. **82**, 73 (1991).

[23] R. Trivedi, M. Radulaski, K. A. Fischer, S. Fan, and J. Vučković, Phys. Rev. Lett. **122**, 243602 (2019).
[24] M. Lukin, M. Fleischhauer, and A. Imamoğlu, *Directions in Quantum Optics* (Springer, Berlin, 2001), pp. 193–203.
[25] J. F. Poyatos, J. I. Cirac, and P. Zoller, Phys. Rev. Lett. **77**, 4728 (1996).
[26] B. Kraus, H. P. Büchler, S. Diehl, A. Kantian, A. Micheli, and P. Zoller, Phys. Rev. A **78**, 042307 (2008).
[27] C. A. Muschik, E. S. Polzik, and J. I. Cirac, Phys. Rev. A **83**, 052312 (2011).
[28] Y.-D. Wang and A. A. Clerk, Phys. Rev. Lett. **110**, 253601 (2013).
[29] P. Zanardi and L. Campos Venuti, Phys. Rev. Lett. **113**, 240406 (2014).
[30] C. Arenz and A. Metelmann, Phys. Rev. A **101**, 022101 (2020).
[31] F. Reiter and A. S. Sørensen, Phys. Rev. A **85**, 032111 (2012).
[32] M. Tavis and F. W. Cummings, Phys. Rev. **170**, 379 (1968).
[33] R. H. Lehmberg, Phys. Rev. A **2**, 883 (1970).
[34] U. Akram, Z. Ficek, and S. Swain, Phys. Rev. A **62**, 013413 (2000).
[35] R. Zwanzig, J. Chem. Phys. **33**, 1338 (1960).
[36] R. Bonifacio, P. Schwendimann, and F. Haake, Phys. Rev. A **4**, 302 (1971).
[37] S. Schütz, H. Habibian, and G. Morigi, Phys. Rev. A **88**, 033427 (2013).
[38] D. Hagenmüller, S. Schütz, J. Schachenmayer, C. Genes, and G. Pupillo, Phys. Rev. B **97**, 205303 (2018).
[39] R. A. Horn and C. R. Johnson, *Matrix Analysis*, 2nd ed. (Cambridge University Press, New York, 2012).
[40] C. Cohen-Tannoudji, Phys. Scr. **T12**, 19 (1986).
[41] D. A. Lidar, Z. Bihary, and K. B. Whaley, Chem. Phys. **268**, 35 (2001).
[42] H. J. Carmichael, R. J. Brecha, M. G. Raizen, H. J. Kimble, and P. R. Rice, Phys. Rev. A **40**, 5516 (1989).
[43] D. F. V. James, Phys. Rev. A **47**, 1336 (1993).
[44] Y.-C. Liu, X. Luan, H.-K. Li, Q. Gong, C. W. Wong, and Y.-F. Xiao, Phys. Rev. Lett. **112**, 213602 (2014).
[45] J. E. Ramírez-Muñoz, J. P. Restrepo Cuartas, and H. Vinck-Posada, Phys. Lett. A **382**, 3109 (2018).
[46] N. Shammah, S. Ahmed, N. Lambert, S. De Liberato, and F. Nori, Phys. Rev. A **98**, 063815 (2018).
[47] A. Canaguier-Durand, C. Genet, A. Lambrecht, T. W. Ebbesen, and S. Reynaud, Eur. Phys. J. D **69**, 24 (2015).
[48] T. Neuman and J. Aizpurua, Optica **5**, 1247 (2018).
[49] M. Reitz, C. Sommer, and C. Genes, Phys. Rev. Lett. **122**, 203602 (2019).
[50] M. Berry, Czech. J. Phys. **54**, 1039 (2004).
[51] T. Gao, G. Li, E. Estrecho, T. C. H. Liew, D. Comber-Todd, A. Nalitov, M. Steger, K. West, L. Pfeiffer, D. W. Snoke, A. V. Kavokin, A. G. Truscott, and E. A. Ostrovskaya, Phys. Rev. Lett. **120**, 065301 (2018).
[52] F. Herrera and F. C. Spano, Phys. Rev. Lett. **116**, 238301 (2016).
[53] J. Flick, M. Ruggenthaler, H. Appel, and A. Rubio, Proc. Natl. Acad. Sci. USA **114**, 3026 (2017).
[54] R. F. Ribeiro, L. A. Martínez-Martínez, M. Du, J. Campos-Gonzalez-Angulo, and J. Yuen-Zhou, Chem. Sci. **9**, 6325 (2018).
[55] S. Kéna-Cohen and J. Yuen-Zhou, ACS Cent. Sci. **5**, 386 (2019).